Radiophysics and Quantum Electronics, Vol. 43, No. 10, 2000

AMBIGUITY OF THE RECONSTRUCTION OF PLASMA FREQUENCY PROFILES FROM A GIVEN HEIGHT–FREQUENCY CHARACTERISTIC AND THEIR DISCERNIBILITY FOR OBLIQUE PROPAGATION OF HF RADIO WAVES IN AN ISOTROPIC IONOSPHERE

S. Ya. Mikhailov

UDC 621.371; 550.388.2

We specify the formulation of the problem of reconstructing the plasma frequency height distribution from a given height–frequency characteristic (HFC) for a spherically symmetric isotropic ionosphere. We propose a numerical algorithm for solving the problem of correctly processing the region of near-critical frequencies of ionospheric layers. On this basis, we study the discernibility of plasma frequency profiles (PFPs) satisfying a given HFC when the properties of an obliquely propagating HF signal are analyzed.

1. INTRODUCTION

The objective of this paper is to estimate the discernibility of PFPs among the family of profiles satisfying a given HFC when the properties of an obliquely propagating HF signal are analyzed. This estimate is required, for example, to explain the unsuccessful numerical experiments on simulation of oblique ionograms obtained by invoking ionosphere models adapted using vertical sounding data. Such an estimate is also necessary for studying the possibility of unambiguously reconstructing the spatial plasma–frequency distribution by joint use of vertical and oblique ionosphere sounding data.

To reconstruct PFPs from a HFC, we wanted at first to use the well-known methods proposed by the recognized authors. However, when we got to know these methods and tested them on a computer, we saw their one important drawback —the absence of a distinct definition of a layer maximum height. That is why frequency step splitting (rigorously infinite splitting) is required when setting HFC near the critical frequency [1], and the maximum heights of the layers are determined using extrapolation formulas [1], which is not correct. This problem cannot be resolved in terms of the piecewise-parabolic approximation of the reflection height proposed in [2]. The simplest way is by using a parabolic approximation of the square of the plasma frequency (electron density) near the layer maximum, but in the above methods this leads to the occurrence of divergent integrals determining the true reflection height at the critical frequency of the layer. Such a situation results from the incorrect formulation of the problem of PFP reconstruction near the critical frequency because of the use of the expression for the signal delay following from the geometric-optics method which is not valid near the critical frequency. The resulting set of extrapolation definitions of a layer maximum height is represented well in [3].

In connection with this, we specify the formulation of the problem of reconstructing the plasma frequency profile from a given HFC to find the correct solution at the critical frequencies of the layers. On this basis, we devise an algorithm for complete solution of this problem in terms of a spherically symmetric isotropic ionosphere model in the absence of absorption. This reconstruction algorithm is used to study the discernibility of the PFP among the family of profiles satisfying a given HFC when the properties of

Institute of Solar–Terrestrial Physics, Siberian Branch of the Russian Academy of Sciences, Irkutsk, Russia.
Translated from Izvestiya Vysshikh Uchebnykh Zavedenii, Radiofizika, Vol. 43, No. 10, pp. 855–872, October, 2000. Original article submitted June 14, 2000.

 0033-8443/00/4310-0766$25.00

an obliquely propagating HF signal are analyzed. To formulate more accurately the PFP reconstruction problem, we will use the results of studies of radio wave reflection from a multilayer isotropic ionosphere in the regions of near-critical frequencies on the basis of the standard-equation method [4]. The characteristics of obliquely propagating HF signals are calculated in terms of the normal-wave method [5].

2. FORMULATION OF THE PROBLEM

To formulate the PFP reconstruction problem, one must determine the expression for direct calculation of the effective phase height or effective group height. This can be done on the basis of the equations derived in [4] by equating the spectral parameter γ to zero ($\gamma = \cos\beta$, where β is the radiation angle). We will choose a somewhat different way to represent consistently the calculation formulas and calculation rules. Among the formulas given in [4], we wlll make use of only those for the spatial phase increment of the signal, and we will obtain formulas for the effective group height by phase differentiation with respect to the frequency.

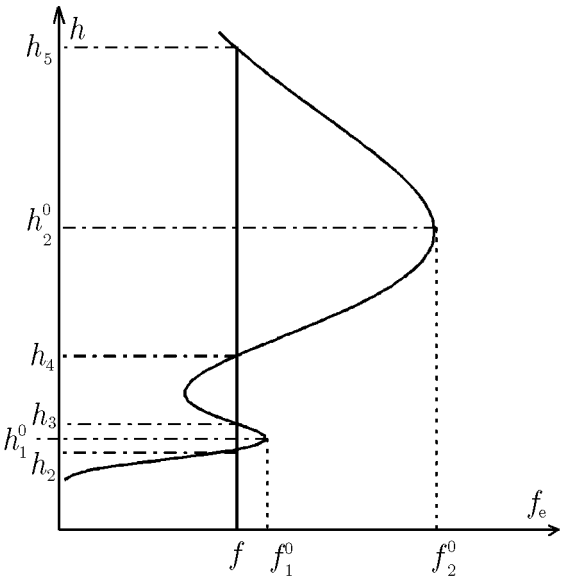

Fig. 1. Vertical profile of the plasma frequency.

For definiteness, we assume that the ionosphere has two layers. The profile of the plasma frequency f_e is shown qualitatively in Fig. 1 where we also define the designations required for the further analysis. At the signal frequency f indicated in this figure all the turning points are real. However, the turning points h_2 and h_3 become complex for $f > f_1^0$, and the turning points h_4 and h_5 become complex for $f > f_2^0$. According to [4], the halves of the spatial phase increments of the modes reflected from the first P_E and second P_F layers can be represented as

$$P_E = k\int\limits_0^{\tilde{h}_2} \sqrt{\varepsilon}\,\mathrm{d}h + \mathrm{Re}[\tilde{\Psi}_2(kb_1)],$$

$$P_F = k\int\limits_0^{\tilde{h}_2} \sqrt{\varepsilon}\,\mathrm{d}h + k\int\limits_{\tilde{h}_3}^{\tilde{h}_4} \sqrt{\varepsilon}\,\mathrm{d}h + 2\,\mathrm{Re}[\tilde{\Psi}_1(kb_1)] + \mathrm{Re}[\tilde{\Psi}_2(kb_2)], \qquad (1)$$

where k is the wave number in vacuum and the dielectric permittivity ε is given by $1 - f_e^2(h)/f^2$. The functions of the following integrals stand under the sign of the real part:

$$b_{1,2} = \frac{i}{\pi}\int\limits_{h_{2,4}}^{h_{3,5}} \sqrt{\varepsilon}\,\mathrm{d}h. \qquad (2)$$

The integration limits are $\tilde{h}_2 = h_2$ and $\tilde{h}_3 = h_3$ for $b_1 \geq 0$ ($f \leq f_1^0$), $\tilde{h}_2 = \tilde{h}_3 = \hat{h}_1$ for $b_1 < 0$ ($f > f_1^0$), $\tilde{h}_4 = h_4$ for $b_2 \geq 0$ ($f \leq f_2^0$), and $\tilde{h}_4 = \hat{h}_2$ for $b_2 < 0$ ($f > f_2^0$); $\hat{h}_{1,2}$ are the solutions of the following equations:

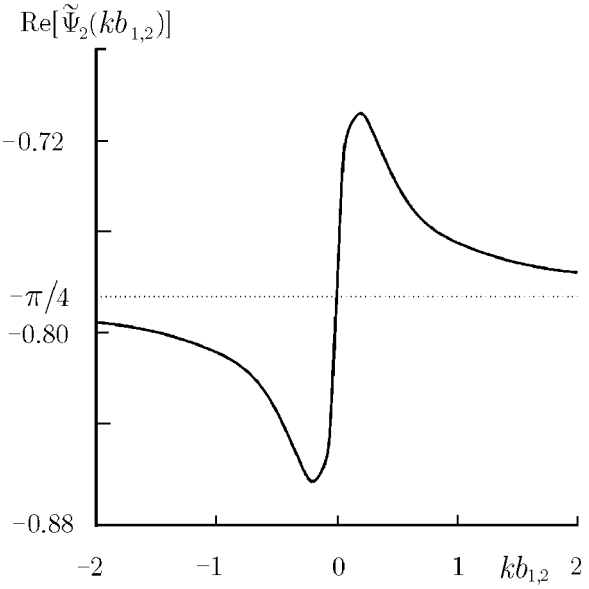

Fig. 2. Half-phases of the reflection coefficients for the first- and second-layer maxima.

$$\int\limits_{h_{2,4}}^{\hat{h}_{1,2}} \sqrt{\varepsilon}\,\mathrm{d}h = \frac{1}{2}\int\limits_{h_{2,4}}^{h_{3,5}} \sqrt{\varepsilon}\,\mathrm{d}h.$$

The functions $\tilde{\Psi}_2(kb_{1,2})$ and $\tilde{\Psi}_1(kb_1)$ are calculated using the formulas

$$\tilde{\Psi}_1(kb_1) = \frac{1}{2i}\,\mathrm{Ln}[T_\mathrm{i}^0(kb_1)],$$

$$\tilde{\Psi}_2(kb_{1,2}) = \frac{1}{2i}\,\mathrm{Ln}[V_\mathrm{i}^0(kb_{1,2})],$$

where the arguments of the logarithms are the reflection coefficient from the first-layer maximum $V_\mathrm{i}^0(kb_1)$, the reflection coefficient from the second-layer maximum $V_\mathrm{i}^0(kb_2)$, and the transmission coefficient of the first-layer maximum $T_\mathrm{i}^0(kb_1)$. For T_i^0 and V_i^0, the design formulas have the form

$$T_\mathrm{i}^0(kb_1) = ie^{-\pi kb_1}V_\mathrm{i}^0(kb_1),$$

$$V_\mathrm{i}^0(kb_{1,2}) = \begin{cases} e^{-\pi kb_{1,2}}V_\mathrm{i}(kb_{1,2}), & b_{1,2} \le 0; \\ V_\mathrm{i}(kb_{1,2}), & b_{1,2} \ge 0, \end{cases}$$

$$V_\mathrm{i}(kb_{1,2}) = \frac{\sqrt{2\pi}\exp[-i\pi/2 - ikb_{1,2}\,\mathrm{Ln}(e^{-i\pi/2}kb_{1,2}/e)]}{(1+e^{-2\pi kb_{1,2}})\,\Gamma(1/2 - ikb_{1,2})},$$

where $\Gamma(x)$ is a gamma function. The half-phase of the transmission coefficient of the first-layer maximum $\mathrm{Re}[\tilde{\Psi}_1(kb_1)]$ changes considerably near zero as kb_1 changes from -1 to 1. The half-phases of the reflection coefficients for the first- and second-layer maxima $\mathrm{Re}[\tilde{\Psi}_2(kb_{1,2})]$ change considerably near the value $-\pi/4$ for $kb_{1,2} \in [-1, 1]$. The diagram $\mathrm{Re}[\tilde{\Psi}_2(kb_{1,2})]$ is represented in Fig. 2, and $\mathrm{Re}[\tilde{\Psi}_1(kb_1)] = \mathrm{Re}[\tilde{\Psi}_2(kb_1)] + \pi/4$.

By making use of the parabolic approximation near the layer maxima,

$$f_e^2(h) = -a_{1,2}^0\left(h - h_{1,2}^0\right)^2 + \left(f_{1,2}^0\right)^2, \quad a_{1,2}^0 = \left(\frac{2f_{1,2}^0}{l_{1,2}^0}\right)^2, \tag{3}$$

where $l_{1,2}^0$ is the thickness of the layers, one can obtain the following expressions for $b_{1,2}$ on the basis of Eq. (2):

$$b_{1,2} = \frac{\left(f_{1,2}^0\right)^2 - f^2}{2f\sqrt{a_{1,2}^0}}. \tag{4}$$

Equating $kb_{1,2}$ to unity, we find from Eq. (4) the following estimate for the half-intervals of the near-critical frequencies:

$$\Delta f_{1,2}^0 = \frac{c}{\pi l_{1,2}^0} \approx 1\,\mathrm{kHz}/l_{1,2}^0\,[\mathrm{hdrs.\,km}], \tag{5}$$

where c is the velocity of light. This means that the phases of the reflection and transmission coefficients of the layer maxima change considerably in only the frequency intervals $f \in [f_{1,2}^0 - \Delta f_{1,2}^0,\, f_{1,2}^0 + \Delta f_{1,2}^0]$. We find that $l_1^0 \approx 100$ km for the E-layer and $l_2^0 \approx 300$ km for the F-layer; hence, according to Eq. (5), $\Delta f_1^0 \approx 1$ kHz and $\Delta f_2^0 \approx 333$ Hz. Although the intervals of the near-critical frequencies are fairly small, the changes in $\mathrm{Re}[\tilde{\Psi}_{1,2}]$ must necessarily be taken into account for the formulation of inverse problems.

The modulus of the reflection coefficient from the first layer $|V_{\rm i}^0(kb_1)|$ rapidly decreases for $f > f_1^0$ and is approximately equal to $\exp(-\pi)$ even for $f = f_1^0 + \Delta f_1^0$. Hence, the mode reflected from the first layer can be assumed detectable for $0 < f \le f_1^0 + \Delta f_1^0$.

The modulus of the transmission coefficient of the first-layer maximum $|T_{\rm i}^0(kb_1)|$ for $f = f_1^0 - \Delta f_1^0$ is approximately equal to $\exp(-\pi)$ and rapidly increases up to unity with increasing frequency. The modulus of the reflection coefficient from the second layer $|V_{\rm i}^0(kb_2)|$ rapidly decreases with increase in frequency for $f > f_2^0$ and is, in order of magnitude, equal to $\exp(-\pi)$ for $f = f_2^0 + \Delta f_2^0$. Hence, the mode reflected from the second layer must be taken into account in the frequency interval $f_1^0 - \Delta f_1^0 < f < f_2^0 + \Delta f_2^0$.

Taking all this into account, one can write the following expressions for the effective phase heights $h_{\rm ph}^E = P_E/k$ and $h_{\rm ph}^F = P_F/k$ of the first and second layer, respectively:

$$h_{\rm ph}^E = \int\limits_0^{\tilde h_2} \sqrt{\varepsilon}\,{\rm d}h + \frac{1}{k}\,{\rm Re}[\tilde\Psi_2(kb_1)], \quad 0 < f \le f_1^0 + \Delta f_1^0;$$

$$h_{\rm ph}^F = \int\limits_0^{\tilde h_2} \sqrt{\varepsilon}\,{\rm d}h + \int\limits_{\tilde h_3}^{\tilde h_4} \sqrt{\varepsilon}\,{\rm d}h + \frac{2}{k}\,{\rm Re}[\tilde\Psi_1(kb_1)] + \frac{1}{k}\,{\rm Re}[\tilde\Psi_2(kb_2)], \quad f_1^0 - \Delta f_1^0 < f < f_2^0 + \Delta f_2^0. \qquad (6)$$

For given frequency dependences $h_{\rm ph}^E(f)$ and $h_{\rm ph}^F(f)$, expressions (6) determine integral equations with respect to the function $f_e(h)$. Here, $h_{\rm ph}^E(f)$ and $h_{\rm ph}^F(f)$ and, as is shown below, their derivatives are continuous functions in the above frequency intervals.

The expressions for effective group heights can be obtained on the basis of general formulas: $h_{\rm G}^E = (2\pi)^{-1} c\,{\rm d}P_E/{\rm d}f$ for the first layer and $h_{\rm G}^F = (2\pi)^{-1} c\,{\rm d}P_F/{\rm d}f$ for the second layer. Using Eq. (1), we find

$$h_{\rm G}^E = \int\limits_0^{\tilde h_2} \frac{{\rm d}h}{\sqrt{\varepsilon}} + {\rm Re}[\tilde\Psi_2'(kb_1)]\,\frac{{\rm d}(fb_1)}{{\rm d}f}\,,$$

$$h_{\rm G}^F = \int\limits_0^{\tilde h_2} \frac{{\rm d}h}{\sqrt{\varepsilon}} + \int\limits_{\tilde h_3}^{\tilde h_4} \frac{{\rm d}h}{\sqrt{\varepsilon}} + 2\,{\rm Re}[\tilde\Psi_1'(kb_1)]\,\frac{{\rm d}(fb_1)}{{\rm d}f} + {\rm Re}[\tilde\Psi_2'(kb_2)]\,\frac{{\rm d}(fb_2)}{{\rm d}f}\,, \qquad (7)$$

where the primes denote derivatives with respect to the argument. Outside the above intervals of near-critical frequencies, the values $\tilde\Psi_{1,2}'$ are exponentially small, and expressions (7) completely coincide with the values which follow from the geometric-optics method. As the integrals in Eq. (7), the dependences ${\rm Re}[\tilde\Psi_{1,2}']$ have logarithmic singularities in the regions of near-critical frequencies; hence, the limit transition is required here.

According to [5], the behavior of ${\rm Re}[\tilde\Psi_{1,2}']$ in the intervals of near-critical frequencies is determined by the following approximate formulas:

$${\rm Re}[\tilde\Psi_{1,2}'(kb_{1,2})] \approx -\frac{1}{2}\,{\rm Ln}\,|kb_{1,2}| + {\rm Re}[J_2(0)], \quad |kb_{1,2}| \ll 1;$$

$${\rm Re}[J_2(0)] = \frac{\Gamma'(1/2)}{2\Gamma(1/2)} = -0.981\,755. \qquad (8)$$

This approximation neglects of the weak dependence of J_2 on $kb_{1,2}$. For the plasma frequency near the layer maxima, one can use the parabolic approximation (3). Then expressions (4) are valid for $b_{1,2}$. On the basis of these expressions, we find ${\rm d}(fb_{1,2})/{\rm d}f = -f\Big/\sqrt{a_{1,2}^0}$. With allowance for this expression and Eq. (8), the corrections for the effective group path (7) in the regions of near-critical frequencies can be represented as

$$\mathrm{Re}[\tilde{\Psi}'_{1,2}(kb_{1,2})]\frac{\mathrm{d}(fb_{1,2})}{\mathrm{d}f} = \frac{f}{\sqrt{a^0_{1,2}}}\,\mathrm{Ln}\,\frac{\chi_{1,2}}{2\,\delta h^0_{1,2}}\,, \tag{9}$$

where

$$\chi_{1,2} = \sqrt{\left|(f^0_{1,2})^2 - f^2\right|/a^0_{1,2}}, \quad \delta h^0_{1,2} = \frac{\sqrt{c}\,q_2}{2\,\sqrt{\pi}\,(a^0_{1,2})^{1/4}}\,, \quad q_2 = \exp\{\mathrm{Re}[J_2(0)]\} = 0.374\,653.$$

From here, it follows explicitly that for $f \to f^0_{1,2}$ these corrections tend to $-\infty$ since $\chi_{1,2} \to 0$.

At the same time, using Eq. (3), it can easily be shown that the integrals in Eq. (7) at the critical frequencies tend to $+\infty$. The heights h^E_G and h^F_G in the regions of near-critical frequencies can be calculated by extracting the divergent parts of the integrals in Eq. (7) near the layer-maximum heights, i.e., at the heights $h \in \{[\tilde{h}_2 - \delta h_1, \tilde{h}_2], [\tilde{h}_3, \tilde{h}_3 + \delta h_1,], [\tilde{h}_4 - \delta h_2, \tilde{h}_4]\}$. We recall that $\tilde{h}_2 = h_2$, $\tilde{h}_3 = h_3$, and $\tilde{h}_4 = h_4$ for $f < f^0_{1,2}$ and $\tilde{h}_2 = \tilde{h}_3 = h^0_1$ and $\tilde{h}_4 = h^0_2$ for $f \in [f^0_{1,2}, f^0_{1,2} + \Delta f^0_{1,2}]$, respectively. The latter follows from the solution of the above equations for $\hat{h}_{1,2}$ with the invoking of approximation (3).

For the divergent parts of the integrals in Eq. (7) for $f \in [f^0_{1,2} - \Delta f^0_{1,2}, f^0_{1,2} + \Delta f^0_{1,2}]$ with allowance for Eq. (3), one can easily obtain the expressions

$$\int\limits_{\tilde{h}_{2,4}-\delta h_{1,2}}^{\tilde{h}_{2,4}} \frac{\mathrm{d}h}{\sqrt{\varepsilon}} = -\frac{f}{\sqrt{a^0_{1,2}}} \begin{cases} \mathrm{Ln}\,\dfrac{\chi_{1,2}}{\sqrt{2\chi_{1,2}\,\delta h_{1,2} + (\delta h_{1,2})^2} + \delta h_{1,2} + \chi_{1,2}}\,, & f \le f^0_{1,2}; \\ \mathrm{Ln}\,\dfrac{\chi_{1,2}}{\sqrt{\chi^2_{1,2} + (\delta h_{1,2})^2} + \delta h_{1,2}}\,, & f > f^0_{1,2}. \end{cases} \tag{10}$$

For the integral at the limits $[\tilde{h}_3, \tilde{h}_3 + \delta h_1]$, the expression on the right-hand side of Eq. (10) with indices equal to unity is valid. The quantities $\delta h_{1,2}$ can be changed so as to make the sum of Eqs. (9) and (10) equal to zero. From this condition, we find the following equations:

$$\begin{aligned} &\sqrt{2\chi_{1,2}\,\delta h_{1,2} + (\delta h_{1,2})^2} + \delta h_{1,2} + \chi_{1,2} = 2\,\delta h^0_{1,2}, && f \le f^0_{1,2}; \\ &\sqrt{\chi^2_{1,2} + (\delta h_{1,2})^2} + \delta h_{1,2} = 2\,\delta h^0_{1,2}, && f > f^0_{1,2}. \end{aligned}$$

These equations are solved by means of simple transformations, and for $\delta h_{1,2}$ we find

$$\delta h_{1,2} = \begin{cases} \dfrac{(2\,\delta h^0_{1,2} - \chi_{1,2})^2}{4\,\delta h^0_{1,2}}\,, & f \in [f^0_{1,2} - \Delta f_{1,2}, f^0_{1,2}]; \\ \dfrac{4\,(\delta h^0_{1,2})^2 - \chi^2_{1,2}}{4\,\delta h^0_{1,2}}\,, & f \in [f^0_{1,2}, f^0_{1,2} + \Delta f_{1,2}]. \end{cases} \tag{11}$$

On the basis of Eq. (11), one can characterize the behavior of $\delta h_{1,2}$ as follows: $\delta h_{1,2}$ are nonzero in the frequency intervals $f \in [f^0_{1,2} - \Delta f_{1,2}, f^0_{1,2} + \Delta f_{1,2}]$, and $\Delta f_{1,2}$ are determined by the equations $2\,\delta h^0_{1,2} - -\chi_{1,2} = 0$. Hence, for $\Delta f_{1,2}$ we obtain the expressions

$$\Delta f_{1,2} \approx \frac{2a^0_{1,2}\,(\delta h^0_{1,2})^2}{f^0_{1,2}} = \frac{cq_2^2}{\pi l^0_{1,2}} \approx 0.140\,4\,\mathrm{kHz}/l^0_{1,2}\,[\mathrm{hdrs.\,km}], \tag{12}$$

which are smaller by a factor of q_2^2 than the half-intervals of the near-critical frequencies determined in Eq. (5) and take the approximate values $\Delta f_1 \approx 140$ Hz and $\Delta f_2 \approx 46$ Hz. At the ends of these frequency intervals, $\delta h_{1,2} = 0$. At the critical frequencies, the values $\delta h_{1,2}$ reach maxima, so that

$$\delta h_{1,2} = \delta h_{1,2}^0 = q_2 \sqrt{\frac{c l_{1,2}^0}{8\pi f_{1,2}^0}} \approx q_2 \sqrt{\frac{l_{1,2}\,[\text{hdrs. km}]}{f_{1,2}^0\,[\text{MHz}]}}\,[\text{km}]\,, \tag{13}$$

from which we find that $\delta h_1^0 \approx 150{-}400$ m and $\delta h_2^0 \approx 200{-}400$ m. These estimates, which follow from Eqs. (12) and (13), are reliable proof of the correctness of the parabolic approximation (3) used here. Moreover, these estimates justify the approximation (8), which, as follows from Eq. (12), is only used in the interval $|kb_{1,2}| < q_2^2 = 0.140\,4$ within the limits of the monotonic variation of $\mathrm{Re}[\tilde{\Psi}_2(kb_{1,2})]$ (Fig. 2).

After defining $\delta h_{1,2}$ (11), calculation of the effective group heights (7) reduces to the following:

$$\begin{aligned} h_{\mathrm{G}}^E(f) &= \int\limits_0^{\tilde{h}_2-\delta h_1} \frac{\mathrm{d}h}{\sqrt{\varepsilon}}\,, \quad 0 < f \le f_1^0 + \Delta f_1^0; \\ h_{\mathrm{G}}^F(f) &= \int\limits_0^{\tilde{h}_2-\delta h_1} \frac{\mathrm{d}h}{\sqrt{\varepsilon}} + \int\limits_{\tilde{h}_3+\delta h_1}^{\tilde{h}_4-\delta h_2} \frac{\mathrm{d}h}{\sqrt{\varepsilon}}\,, \quad f_1^0 - \Delta f_1^0 \le f \le f_2^0 + \Delta f_2^0, \end{aligned} \tag{14}$$

where

$$\tilde{h}_2 - \delta h_1 = h_2, \quad f \le f_1^0 - \Delta f_1;$$

$$\tilde{h}_3 + \delta h_1 = h_3, \quad f \le f_1^0 - \Delta f_1;$$

$$\tilde{h}_{2,3} \mp \delta h_1 = \begin{cases} h_1^0 \mp \delta h_1^0 \mp \dfrac{\chi_1^2}{4\,\delta h_1^0}\,, & f_1^0 - \Delta f_1 < f \le f_1^0; \\ h_1^0 \mp \delta h_1^0 \pm \dfrac{\chi_1^2}{4\,\delta h_1^0}\,, & f_1^0 < f \le f_1^0 + \Delta f_1; \end{cases}$$

$$\begin{aligned} \tilde{h}_2 - \delta h_1 = \tilde{h}_3 + \delta h_1 = h_1^0, &\quad f > f_1^0 + \Delta f_1; \\ \tilde{h}_4 - \delta h_2 = h_4, &\quad f < f_2^0 - \Delta f_2; \end{aligned}$$

$$\tilde{h}_4 - \delta h_2 = \begin{cases} h_2^0 - \delta h_2^0 - \dfrac{\chi_2^2}{4\,\delta h_2^0}\,, & f_2^0 - \Delta f_2 < f \le f_2^0; \\ h_2^0 - \delta h_2^0 + \dfrac{\chi_2^2}{4\,\delta h_2^0}\,, & f_2^0 \le f < f_2^0 + \Delta f_2. \end{cases}$$

These formulas completely determine the algorithm for direct calculation of h_{G}^E and h_{G}^F for a given two-layer plasma frequency profile. They can easily be generalized to the cases of both one- and three-layer PFP (as well as to the cases of more complex profiles).

In the formulation of the inverse problem, the functions $h_{\mathrm{G}}^E(f)$ and $h_{\mathrm{G}}^F(f)$ are given in the above frequency intervals and are continuous together with their first-order derivatives (this can easily be verified using Eqs. (9) and (10)). Expressions (7) and (14) then determine different forms of representation of integral equations for the function $f_e(h)$ (the representation (7) is more general). The convergence of the functions $h_{\mathrm{G}}^E(f)$ and $h_{\mathrm{G}}^F(f)$ into a unified function $h_{\mathrm{G}}(f)$ indicates the absence of a valley, and the presence of a maximum in $h_{\mathrm{G}}(f)$ indicates the presence of a bend on the PFP. All these conditions are necessary for the solution of the inverse problem.

3. SOLVING THE INVERSE PROBLEM

Let us discuss different methods of solving the inverse problem. The first method is that of seeking the analytical solution in the form of quadratures. Outside the regions of near-critical frequencies, this is reached by reducing integral equations (6) and (7) or (14) to the Abel equation, and then the solution is found using the Abel inversion [6, 7]. In the regions of near-critical frequencies, these integral equations

do not reduce to the Abel equation, and seeking directly their analytical solution encounters considerable difficulties. The second method of solving the integral equations discussed here is associated with numerical techniques. The accuracy of these techniques is determined by postulating the class of functions in which the solution $f_e^2(h)$ is sought. The available numerical methods of solving inverse problems mainly assume seeking $f_e^2(h)$ in the class of continuous functions. These methods ensure satisfactory accuracy everywhere except for the regions of near-critical frequencies where their accuracy is obviously not sufficient.

In what follows we develop a method for numerical solution of integral equations (14) by modifying the Jackson method [8] ($f_e^2(h)$ is a continuous function) with increase in accuracy in the layer maximum regions (near-critical frequencies) and valleys, where $f_e^2(h)$ belongs to the class of functions that are continuous together with their first-order derivatives.

Let the effective group heights $h_{\rm G}^E(f)$ and $h_{\rm G}^F(f)$ be assigned on an arbitrary grid of frequencies f_n, where $n = 1, 2, \ldots, N_2$, by an array of values h'_n with the only constraint that $f_{N_1} = f_{N_1+1} = f_1^0$, $h'_{N_1} = h_{\rm G}^E(f_1^0)$, and $h'_{N_1+1} = h_{\rm G}^F(f_1^0)$ for $n = N_1, N_1+1$ and that $f_{N_2} = f_2^0$ and $h'_{N_2} = h_{\rm G}^F(f_2^0)$ for $n = N_2$. We will seek the true heights $h(f_e)$ on a grid of plasma frequencies f_{e_i} which coincides with the grid of operating frequencies f_n ($f_{e_i} = f_n$ for $i = n$).

Assuming that the ionosphere begins with the height h_0 and the derivative $\mathrm{d}h/\mathrm{d}f_e = \Delta h_i/\Delta f_{e_i}$ is constant in each interval $\Delta f_{e_i} = \Delta f_{e_i} - \Delta f_{e_{i-1}}$, one can replace the first integral in Eq. (14) by the sum of integrals for the values $f = f_n$, where $n = 1, 2, \ldots, (N_1 - 1)$. Then we arrive at the system of equations

$$h'_n = h_0 + \sum_{i=1}^{n} I_{in}, \quad I_{in} = \Delta h_i \, M_{in},$$

$$M_{in} = \frac{1}{\Delta f_{e_i}} \int\limits_{f_{e_{i-1}}}^{f_{e_i}} \frac{\mathrm{d}f_e}{\sqrt{1-(f_e/f_n)^2}} = \frac{f_n}{\Delta f_{e_i}} \arcsin \left\{ \frac{f_{e_i}}{f_n} \sqrt{1 - \frac{f_{e_{i-1}}^2}{f_n^2}} - \frac{f_{e_{i-1}}}{f_n} \sqrt{1 - \frac{f_{e_i}^2}{f_n^2}} \right\}. \tag{15}$$

The solution of these equations in the above interval of the frequency grid can be written in the form of the following algorithm which is central in the Jackson method:

$$h_n = h_0 + \sum_{i=1}^{n} \Delta h_i, \quad \Delta h_n = \Delta \tilde{h}'_n / M_{nn}, \quad \Delta \tilde{h}'_n = h'_n - h_0 - \sum_{i=1}^{n-1} I_{in}. \tag{16}$$

In the first step ($n = 1$), we have $\Delta \tilde{h}'_1 = h'_1 - h_0$, $M_{11} = \pi/2$, and $\Delta h_1 = 2\,(h'_1 - h_0)/\pi$. The stepwise use of Eqs. (16) determines the increments of the true height and the true heights themselves. This permits one to find one solution from the family where the scaling parameter is the zero height h_0 of the ionosphere.

In the integration interval $n = N_1$, the approximation of $f_e(h)$ by a linear function is not valid. The way out is by using the parabolic approximation in Eq. (3) for $f_e^2(h)$. From the joining condition, we find

$$a_1^0 = \frac{(f_1^0)^2 - f_{N_1-1}^2}{(h_{N_1-1} - h_1^0)^2} = \frac{f_{N_1}^2 - f_{N_1-1}^2}{(h_{N_1-1} - h_{N_1})^2}\,. \tag{17}$$

The last element in the sum (15) is now equal to the integral

$$I_{nn} = \int\limits_{h_{N_1-1}}^{h_{N_1} - \delta h_1^0} \frac{\mathrm{d}h}{\sqrt{\varepsilon}} = -\frac{f_{N_1}}{\sqrt{a_1^0}} \operatorname{Ln} \frac{\delta h_1^0}{h_{N_1} - h_{N_1-1}} = \frac{f_{N_1}}{\sqrt{a_1^0}} \operatorname{Ln} \frac{1}{Q\,(a_1^0)^{1/4}}\,, \tag{18}$$

$$Q = \frac{\sqrt{c}\, q_2}{2\sqrt{\pi\,(f_{N_1}^2 - f_{N_1-1}^2)}}\,,$$

which was calculated taking into account Eq. (17) and the expression for δh_1^0 from Eq. (9). The new equation of system (15) can be reduced to the transcendental form

$$e^{-\alpha z} = Q\sqrt{z}, \quad z = \sqrt{a_1^0}, \quad \alpha = \frac{\Delta\tilde{h}'_{N_1}}{f_{N_1}}, \tag{19}$$

determining a_1^0. Then the increment $\Delta h_n = \Delta h_{N_1}$ is found from Eq. (17) and the height of the first-layer maximum is determined by the continuation of the sum (16).

We will seek the solution of Eq. (19) by the differential-parametric method [9]. For this, we assume that $z(t)$ is the solution of the equation

$$e^{-\alpha z} = Q\sqrt{z}\,t. \tag{20}$$

For $t = 1$, Eqs. (20) and (19) coincide; hence, $z(1)$ is simultaneously the solution of Eq. (19). Differentiating Eq. (20) with respect to t and replacing the transcendental function by an algebraic one in the resulting expression in accordance with Eq. (20), one can easily reduce the solution of Eq. (19) to solution of the following Cauchy problem:

$$\frac{\mathrm{d}z}{\mathrm{d}t} = \frac{-z}{(\alpha z + 1/2)\,t}, \quad z(t_0) = z_0, \quad t \in [1, t_0]; \quad t_0 = \frac{\sqrt{\alpha}}{Q\sqrt{j}\,e^j}, \quad z_0 = \frac{j}{\alpha}, \tag{21}$$

where j is the largest integer for which t_0 is still greater than unity. Integration of Eq. (21) by the Runge–Kutta method permits one to find the solution of Eq. (19) on a grid of 7 to 8 decimal nonzero digits with an error of the order of 10^{-6}.

Integration in the interval $n = N_1 + 1$ requires approximating the valley. We will define the valley by two joined parabolas:

$$\begin{aligned} f_e^2(h) &= -a_1\,(h - h_1^0)^2 + (f_1^0)^2, \quad h_1^0 \le h \le h_j; \\ f_e^2(h) &= a_2\,(h - h_v)^2 + f_v^2, \quad h_j \le h \le h_4, \end{aligned} \tag{22}$$

where f_v and h_v are the plasma frequency and the bottom height of the valley and h_j is the height of the joining point of the parabolas. Joining the function $f_e^2(h)$ and its first-order derivative at the first-layer maximum in Eq. (22) has already been reached. We will characterize the asymmetry of the valley by the relation $p = a_2/a_1$. From the condition of joining the first-order derivatives for $h = h_j$ we find

$$h_j = \frac{ph_v + h_1^0}{1+p} = \frac{ph_v + h_{N_1}}{1+p}. \tag{23}$$

For $p \to 0$ and $h_j \to h_1^0$ we obtain a symmetric valley, and for $p \to +\infty$ and $h_j \to h_v$ the valley is most asymmetric. The use of Eq. (23) for joining the dependences f_e^2 at the point h_j makes it possible to determine a_1 in the following manner:

$$a_1 = \frac{(f_1^0)^2 - f_v^2}{(h_v - h_1^0)^2}\frac{1+p}{p} = \frac{f_{N_1}^2 - f_v^2}{(h_v - h_{N_1})^2}\frac{1+p}{p}. \tag{24}$$

With allowance for Eq. (24), the turning point h_4 is found from the second equation (22) under the condition $f_e^2(h_4) = f_{N_1+1}^2$:

$$h_{N_1+1} = h_4 = \frac{h_v - h_1^0}{\sqrt{1+p}} + h_v = \frac{h_v - h_{N_1}}{\sqrt{1+p}} + h_v. \tag{25}$$

Thus, if the plasma frequency of the valley bottom f_v and the asymmetry p are assumed given, then for complete determination of the valley one must find the parameter h_v or a_1. For $n = N_1 + 1$, the last element of the sum (15) in accordance with Eq. (22) is now equal to the sum of integrals

$$I_{nn} = \int\limits_{h_{N_1}+\delta h_1^0}^{h_j} \frac{\mathrm{d}h}{\sqrt{\varepsilon}} + \int\limits_{h_j}^{h_4} \frac{\mathrm{d}h}{\sqrt{\varepsilon}} = \frac{f_{N_1}}{\sqrt{a_1}} \operatorname{Ln} \frac{1}{Q_v (a_1)^{1/4}}\,, \tag{26}$$

$$Q_v = \frac{\sqrt{c}\, q_2 \sqrt{1+1/p}}{2\sqrt{\pi(f_{N_1}^2 - f_v^2)}\, \exp\left[\left(\pi/2 + \arcsin\left(1/\sqrt{1+p}\right)\right)/\sqrt{p}\,\right]}\,,$$

where for the transformation of the right-hand side we used Eq. (24) and the expression for δh_1^0 from Eq. (9). Hence, as in the previous step, the last equation of system (15) reduces to the form

$$e^{-\alpha_v z} = Q_v \sqrt{z}, \quad z = \sqrt{a_1}, \quad \alpha_v = \frac{\Delta \tilde{h}'_{N_1+1}}{f_{N_1}}\,, \quad \Delta \tilde{h}'_{N_1+1} = \Delta h'_n = h'_{N_1+1} - h'_{N_1}, \tag{27}$$

which is completely similar to Eq. (19). Solving Eq. (27) reduces to integrating the Cauchy problem (21) with α replaced by α_v and Q replaced by Q_v. After finding z, the desired parameters are determined as follows: $a_1 = z^2$, $a_2 = pa_1$, $(h_v - h_{N_1})$ is found from Eq. (24), and h_{N_1+1} from Eq. (25).

It should be mentioned that if only continuity of $f_e^2(h)$ is required for escaping the valley at the point $h_4 = h_{N_1+1}$, then a family of solutions with two scaling parameters, f_v and p, will satisfy the formulated problem in the valley region. It is shown below that, by also requiring continuity for the derivative of $f_e^2(h)$ in escaping the valley, one fixes the asymmetry p, which makes it possible to scale the entire family of solutions by one parameter.

Then, for integration in the intervals $n = (N_1 + 2), \ldots, (N_2 - 1)$ approximating $f_e(h)$ by segments of linear functions is valid, and the Jackson method (16) can be followed to determine the true heights. In the integration intervals where the quadratic approximation $f_e^2(h)$ was assumed (i.e., for $i = N_1, N_1 + 1$), the elements of the sum (15) are calculated using the following formulas:

$$\begin{aligned}
I_{N_1 n} &= \frac{f_n}{\sqrt{a_1^0}} \operatorname{Ln} \frac{\sqrt{f_{N_1}^2 - f_{N_1-1}^2} + \sqrt{f_n^2 - f_{N_1-1}^2}}{\sqrt{f_n^2 - f_{N_1}^2}}\,, \\
I_{N_1+1\, n} &= \frac{f_n}{\sqrt{a_1}} \left\{ \operatorname{Ln} \frac{\sqrt{p\,(f_{N_1}^2 - f_v^2)/(1+p)} + \sqrt{p\,(f_{N_1}^2 - f_v^2)/(1+p) + f_n^2 - f_{N_1}^2}}{\sqrt{f_n^2 - f_{N_1}^2}} + \right. \\
&+ \left. \frac{1}{p} \left(\arcsin \frac{\sqrt{f_{N_1+1}^2 - f_v^2}}{\sqrt{f_n^2 - f_v^2}} + \arcsin \frac{\sqrt{f_{N_1+1}^2 - f_v^2}}{\sqrt{(1+p)\,(f_n^2 - f_v^2)}} \right) \right\}\,,
\end{aligned} \tag{28}$$

which are obtained by invoking Eqs. (3) and (22) calculating integrals at the limits $[h_{N_1-1}, h_{N_1}]$ and $[h_{N_1}, h_{N_1+1}]$, respectively, since outside the region of near-critical frequencies $\delta h_1 = 0$. The true heights for $i > N_1 + 1$ are determined in accordance with Eqs. (15) and (16).

In the last integration step ($n = N_2$), one must use the quadratic approximation (3) for $f_e^2(h)$. Then the coefficient a_2^0 is calculated by integrating the Cauchy problem (21), where $\alpha = \Delta \tilde{h}'_{N_2}/f_{N_2}$, $Q = \sqrt{c}\, q_2 \Big/ \left(2\sqrt{\pi(f_{N_2}^2 - f_{N_2-1}^2)}\right)$, and $a_2^0 = z^2$. As in Eq. (17), $\Delta h_{N_2} = h_{N_2} - h_{N_2-1} = \sqrt{f_{N_2}^2 - f_{N_2-1}^2}\Big/ z$, and the height of the second-layer maximum h_{N_2} is determined by the continuation of the sum (16). If continuity of $[f_e^2(h)]'_h$ at the point $h = h_{N_1+1}$ is not required, then the algorithm for solving the inverse problem ends at this stage.

As the parameter scaling the family of solutions above the first-layer maximum, it may be useful to choose the phase height of the valley $\Delta h_{\mathrm{ph}} = h_{\mathrm{ph}}^F(f_1^0) - h_{\mathrm{ph}}^E(f_1^0)$. This parameter substitutes the scaling parameter f_v. Indeed, by invoking Eqs. (22) and (6), we find

$$\Delta h_{\rm ph} = \frac{f_{N_1}^2 - f_v^2}{2 f_{N_1}\sqrt{a_1}} \left[1 + \frac{1}{\sqrt{p}} \left(\frac{\pi}{2} + \arcsin\frac{1}{\sqrt{1+p}}\right)\right].$$

Hence,

$$f_{N_1}^2 - f_v^2 = \frac{2 f_{N_1}\,\Delta h_{\rm ph}\sqrt{a_1}}{1 + \left(\dfrac{\pi}{2} + \arcsin\dfrac{1}{\sqrt{1+p}}\right)\Big/\sqrt{p}}\,, \tag{29}$$

which gives an additional equation for the unknown coefficient a_1 and makes it unnecessary to solve the transcendental equation (27) in the inverse problem. Let us substitute Eq. (29) into Eq. (27). After simple transformations we come to the following result:

$$z = \sqrt{a_1} = \frac{f_{N_1}}{\Delta h'_{N_1+1}} \,{\rm Ln}\, \frac{2\sqrt{2\pi\,\Delta h_{\rm ph}\, f_{N_1}/c}\exp\left[\dfrac{1}{\sqrt{p}}\left(\dfrac{\pi}{2} + \arcsin\dfrac{1}{\sqrt{1+p}}\right)\right]}{q_2\sqrt{\left(1+\dfrac{1}{p}\right)\left[1 + \dfrac{1}{\sqrt{p}}\left(\dfrac{\pi}{2} + \arcsin\dfrac{1}{\sqrt{1+p}}\right)\right]}}\,. \tag{30}$$

Thus, for given $\Delta h_{\rm ph}$ and p one determines the desired coefficient a_1, and the height of escape from the valley is found from Eqs. (24) and (25).

The above algorithm has one significant drawback by admitting solutions that are ambiguous with respect to the plasma frequency for certain given values of f_v and p (or $\Delta h_{\rm ph}$ and p) after escape from the valley, which must be excluded for physical reasons. Such a drawback can be eliminated by requiring continuity of the derivative $[f_e^2(h)]'_h$ at the point $h_4 = h_{N_1+1}$. To satisfy this requirement, one must match derivatives before and after escaping the valley. Before escaping the valley, we find, using Eq. (22), that

$$PR = h'_{f_e^2} = \left(\frac{{\rm d}f_e^2}{{\rm d}h}\right)^{-1} = \frac{1}{2a_2\,(h_4 - h_v)} = \frac{1}{2\sqrt{p a_1\sqrt{f_{N_1+1}^2 - f_v^2}}}\,. \tag{31}$$

After escaping the valley ($n = N_1 + 2$), with allowance for Eqs. (16) and (28), one can write

$$PR_1 = h'_{f_e^2} = \frac{\Delta h_n}{\Delta f_n^2} = \frac{\Delta h_{N_1+2}}{f_{N_1+2}^2 - f_{N_1+1}^2} = \frac{\Delta\tilde{h}'_{N_1+2}}{M_{N_1+2\,N_1+2}\,(f_{N_1+2}^2 - f_{N_1+1}^2)}\,. \tag{32}$$

To match derivatives, one must find p such that $PR_1 - PR = 0$. The solution of this equation can be found numerically by the Newton method [10], repeating many times the integration stages $n = N_1 + 1$ and $n = N_1 + 2$. For this, in the admissible interval of p variation $p \in [0.01; 100]$ the asymmetry is defined by the sequence $p_m = \exp(x_m)$, where $x_m = {\rm Ln}(100)\,(2m/m_0 - 1)$, $m = 0, 1, 2, \ldots, m_0$, and m_0 is a fixed integer, and the integration stages $n = N_1 + 1$ and $n = N_1 + 2$ are repeated until the difference $R_m = PR_1 - PR$ reverses sign. Then the values p change in accordance with the Newton method $p_{m+1} = p_m \exp[-R_m\,(x_m - x_{m-1})/(R_m - R_{m-1})]$ until the difference R_m reaches zero with a given accuracy. After that the solution of the inverse problem is fulfilled in accordance with the above scheme.

Information on the found solution after using this algorithm is contained in the arrays h_n and f_n, where $n = 0, 1, \ldots, N_2$, and in the coefficients of analytical functions (3) and (22): a_1^0, $h \in [h_{N_1-1}, h_{N_1}]$; a_1, $h \in [h_{N_1}, ph]$; a_2, f_v (or $\Delta h_{\rm ph}$); $h \in [h_j, h_{N_1+1}]$; a_2^0, $h \in [h_{N_2-1}, h_{N_2}]$. For most applications, information can be extracted in the form of a sequence of numbers: h_n, f_n ($n = 0, 1, \ldots, N_1$); h_m, $f_m = f_e(h_m)$, calculated using Eqs. (22) at the points $h_m = h_{N_1} + (h_{N_1+1} - h_{N_1})m/m_0$ ($m = 1, 2, \ldots, (m_0 - 1)$), and then h_n, f_n ($n = (N_1 + 1), \ldots, N_2$).

The resulting solutions are scaled by two parameters, h_0 and f_v (or $\Delta h_{\rm ph}$). Below, we study exactly these solutions (which are continuous together with the first-order derivative in escaping the valley). The

narrowing of the family of solutions due to the uncertainty of the zero height of the ionosphere can be reached by defining the effective group heights at the lowest possible frequencies where it can be assumed that $h_{\rm G} \approx h_{\rm ph} \approx h_0$. Hence, in what follows we focus on the study of the solutions scaled by the parameter f_v (or $\Delta h_{\rm ph}$).

4. DISCERNIBILITY OF PLASMA FREQUENCY PROFILES

The above algorithm was implemented on an IBM PC-486 in the FORTRAN language and was tested in the following manner. Initially, the plasma frequency profile was assigned as the sum of two Chapman layers:

$$f_e(h) = \sum_{i=1}^{2} f_i^0 \exp\left[1 - \frac{h - h_i^0}{T_{\rm i}} - \exp\left(-\frac{h - h_i^0}{T_{\rm i}}\right)\right], \tag{33}$$

where $f_1^0 = 2$ MHz, $h_1^0 = 100$ km, $T_1 = 20$ km, $f_2^0 = 6$ MHz, $h_2^0 = 300$ km, and $T_2 = 120$ km (the solid curve in Fig. 3*a*), and was digitized with a 5-km step with respect to the height. Using these data, we calculated the frequency sweeps of the group (the solid curve in Fig. 3*b*) and phase (the curve shown by circles in Fig. 3*c*) heights using Eqs. (6) and (14) on the basis of the algorithm [11]. Note that for $\gamma = 0$ the phase height $h_{\rm ph}$ is related to the adiabatic invariant $\tilde{I}$, or the phase path, and the normal wave number n [11] by the relationships $h_{\rm ph} = a\tilde{I}/2 = \pi n/k$, where a is the Earth's radius. In the case of oblique propagation of the radio signal, the parameters $\tilde{I}$ and n are related to the vertical component of the phase path by similar relationships.

Then, the arrays of group heights on a uniform 60-dot frequency grid for each trace served as input data for solving the inverse problem. Since the zero height of the ionosphere and the plasma frequency of the bottom must be known, the initial PFP is reconstructed at first. The result of reconstruction is shown by circles in Fig. 3*a*. The difference from Eq. (33) did not exceed 0.5%. After that, we reconstructed the PFPs with deeper and shallower valleys, as shown by crosses and diamonds, respectively, in Fig. 3*a*. Then, the PFPs obtained on a uniform frequency grid were scaled to a uniform height grid, and direct calculation of the frequency sweeps of group and phase heights was performed again on the basis of the algorithm [11]. The results of calculations are presented in Fig. 3*b, c* by symbols corresponding to those used for the designation of PFPs. The difference between the effective group heights did not exceed 1% at all frequencies except the critical frequency, at which the difference reached 2%. This can be the consequence of errors that are unavoidable at the stage of scaling of data to a uniform height grid. The difference of phase heights for the initial profile and the profile shown by circles did not exceed 0.5%. All this is indicative of the high reliability of the algorithm for solving the inverse problem. The PFPs reconstructed in Fig. 3*a* belong to the family of profiles satisfying one HFC (Fig. 3*b*). Choosing one profile from the family requires additional information. As such information, it seems reasonable to use the frequency sweeps of phase heights (Fig. 3*c*), but the absolute value of the spatial increment cannot be measured in the vertical sounding of the ionosphere. Hence, other criteria are necessary to obtain a unique solution of the inverse problem.

Because of the absence of a rigorous modification of the Smith method [12] for the case of a sperically layered ionosphere [13], it should be expected that PFPs satisfying one height–frequency characteristic are discernible in the characteristics of an obliquely propagating signal (we recall that the Smith method for a plane-layered medium solves the problem of direct scaling of HFCs to characteristics of an obliquely propagating signal without the PFP reconstruction). Hence, for the unambiguous solution of the diagnostic problem it can be useful to use joint vertical and oblique ionosphere sounding data.

To check this possibility, we calculated the distance (at the signal frequency f=12 MHz) and frequency (at the distance $D = 2\,000$ km) sweeps of the main characteristics of the signal for a spherically layered nonabsorbing ionosphere defined successively by the plasma frequency profiles shown in Fig. 3*a*. The results of calculations for the $1F$ mode are represented in Fig. 4, where $\tilde{I}$ is an adiabatic invariant, β is the arrival (escape) angle, $\tilde{\tau} = \tau - D/c$, τ is the propagation time, and E_φ is the azimuthal component of the electric field excited by a point vertical magnetic dipole (the height of the emission and observation points is 20 m).

The solid curves denote the results of calculations for the reconstructed initial profile, and the crosses and diamonds stand for the profiles shown by the same symbols in Fig. 3*a*.

From the results presented in Fig. 4 it follows that the signal delays in Fig. 4*c, c′* are the same for the three profiles of the family presented in Fig. 3*a*. The profiles of the family are discernible in the arrival angles β in Fig. 4*b, b′*, but the difference is very small and does not exceed 0.5°. When this information is used to choose the unique solution, rigid requirements, which are difficult to meet in practice, are imposed on the accuracy of angle measurements. The weak dependence of the distance–angle or distance–frequency characteristics on the profile of the family is also not manifested in the signal amplitudes E_φ (Fig. 4*d, d′*), although the derivative of the distance–angle characteristics is used here for the calculation of E_φ. The only characteristic which is really sensitive to the profile of the family is $\tilde{I}$ (Fig. 4*a, a′*), or the phase path, but the absolute value of the spatial phase increment of the signal cannot be measured immediately in the oblique sounding of the ionosphere. Thus, the problem of choosing the unique profile among the family of profiles remains open in this case. At the same time, it follows from the above that the existing modifications of the Smith method for the case of a spherically layered ionosphere can be replaced by the calculation scheme implemented here with the reconstruction of one arbitrary PFP from the family.

The results obtained for a spherically layered ionosphere can be generalized to the case of a three-dimensional inhomogeneous medium. The basis for such a statement is given by the adiabatic approximation of the normal-wave method, according to which [14] the signal parameters on the inhomogeneous path are determined by integrating signal characteristics in comparison waveguides over the propagation path length (along the Earth's surface) for a constant value of the adiabatic invariant. Therefore, if the normalized signal characteristics in each comparison waveguide are shifted to equal values along the invariant axis, then the integration result will remain the same with respect to the distance. This means that there is a family of inhomogeneous media that are undiscernible or only weakly discernible in the case of oblique sounding of the ionosphere. To estimate the discernibility of these media in terms of the main characteristics of an obliquely propagating signal, we performed the following simulation.

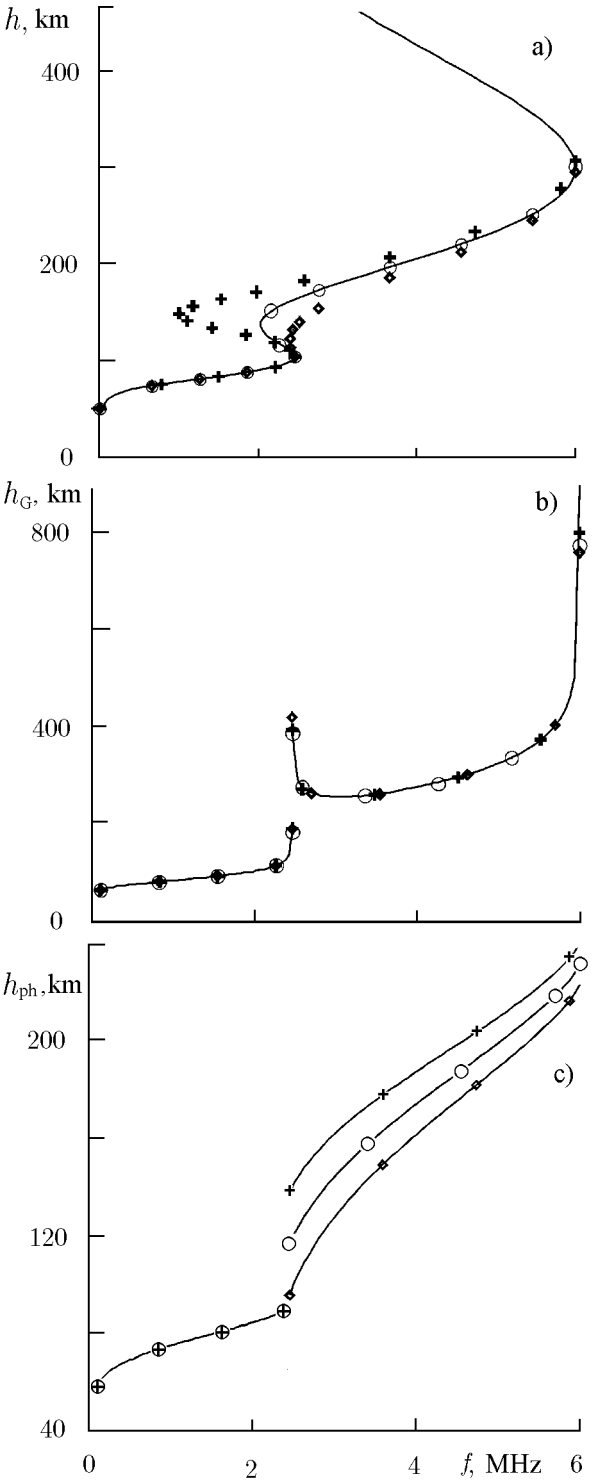

Fig. 3. Plasma frequency profiles (*a*), frequency sweeps of group (*b*), and phase heights (*c*).

On a longitudinally inhomogeneous path of length 2 000 km in five sections with a 500-km step, the two-layer ionosphere was determined by the sum of Chapman layers (33) with the parameters changing along the path in accordance with Table 1. The initial PFPs are shown by solid curves on the left in Fig. 5. The frequency sweeps of the effective group and phase heights calculated on the basis of [11] using these

PFPs are shown by solid curves on the right in Fig. 5. Then, from the HFC in each section we reconstructed PFPs with the phase heights of the valleys $\Delta h_{\rm ph}$ increased to the same value, equal to 30 km, for all the sections. The reconstructed PFPs are shown by dashed curves on the left in Fig. 5. The effective group and phase heights calculated from these profiles are shown on the right in Fig. 5 by crosses and dashed curves, respectively. Thus, we constructed two media satisfying identical HFCs in each section.

Table 1

D, km	f_1^0, MHz	h_1^0, km	T_1, km	f_2^0, MHz	h_2^0, km	T_2, km
0	3.00	90.0	20	6.0	300	120
500	2.25	92.5	20	7.5	295	120
1000	2.00	95.0	20	8.0	290	120
1500	2.25	97.5	20	7.5	285	120
2000	3.00	100.0	20	6.0	280	120

To estimate the discernibility of these media on the basis of [11], we calculated the distance (at the signal frequency 12 MHz) and frequency (at a distance of 2 000 km) sweeps of the main characteristics of individual propagation modes. The results are represented in Fig. 6 with one change in the parameter designation compared with Fig. 4: β_0 is the escape angle and β is the arrival angle. The circles denote the results of calculations for the medium determined by solid profiles and the crosses correspond to dashed profiles in Fig. 5. We examine the characteristics of the modes of the F channel.

From the results represented in Fig. 6 it follows that qualitatively the discernibility of inhomogeneous media remained the same as the spherically layered media. The delays of the F modes $\tilde{\tau}$ coincide well, as previously, in both media. In the escape β_0 and arrival angles β the discernibility of longitudinally inhomogeneous media has been slightly improved, but the difference in angles is still no greater than one degree. This also increased the difference in the signal amplitudes E_φ. Such a difference indicates the change in the focusing properties of the media since the absorption was neglected in the calculations. Despite the improvements, the discernibility of the inhomogeneous media remained weak in the parameters β_0, β, $\tilde{\tau}$, and E_φ. The parameter $\tilde{I}$, or the phase path, remains the most informative parameter for choosing the unique medium from the family. In conclusion we note that the discernibility of media in the signal amplitudes increases considerably if absorption is taken into account, but the use of this fact for diagnostics of the medium is complicated by the necessity of solving the reconstruction problem for the collision frequency profile. However, this problem is outside the scope of this study.

5. CONCLUSIONS

On the basis of these results, the following conclusions can be drawn. In an isotropic two-layer ionosphere, one HFC is satisfied by the family of PFPs scaled by two parameters, h_0 and f_v. The first scaling parameter, h_0, can take values from zero to $h_G^E(f_1)$, where f_1 is the lowest sounding frequency. The second scaling parameter, f_v, can take values from zero to $f_1^0 - \Delta f_1^0$. In this case, the height uncertainty of the valley can reach 100 km and the height uncertainty of the second-layer maximum reaches 60 km, or 20% of its average value. In a spherically layered nonabsorbing ionosphere, the plasma frequency profiles which form a family owing to the above uncertainty are discernible only weakly in the parameters β, $\tilde{\tau}$, and E_φ of an obliquely propagating signal. In the case of an inhomogeneous nonabsorbing ionosphere, there is a family of media which are discernible only weakly in the parameters β_0, β, $\tilde{\tau}$, and E_φ of an obliquely propagating signal. This family of media is scaled by changing the phase heights of the valleys to identical values in each section of the propagation path. The most informative parameter for choosing the unique PFP (or the unique medium on an inhomogeneous path) is the phase path (or the spatial phase increment), but this parameter cannot be measured in the ionosphere sounding. The weak discernibility of the PFP of the family in the parameters β, $\tilde{\tau}$, and E_φ of an obliquely propagating signal is the consequence of the sphericity of the ionosphere, since in a plane-layered medium the problem of scaling HFC to the parameters β, $\tilde{\tau}$, and E_φ can be solved without the PFP reconstruction, in accordance with the Smith method.

To decrease the ambiguity of reconstruction of PFPs satisfying a given HFC, one can use their discernibility in the arrival angles of an obliquely propagating signal. However, one must measure arrival angles with an accuracy of up to several one-hundredths of a degree.

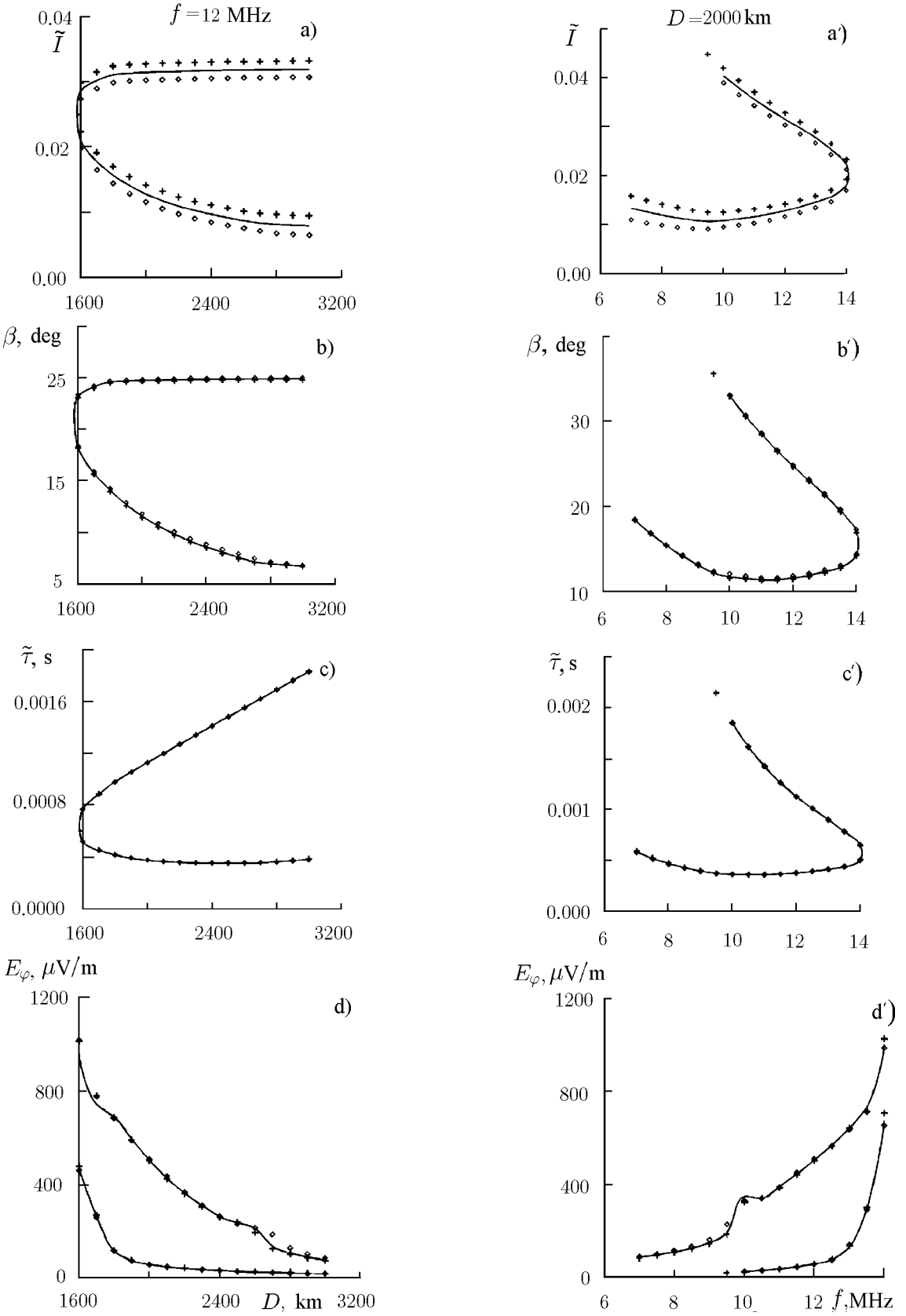

Fig. 4. Distance and frequency sweeps of the main characteristics of the $1F$ mode on a spherically symmetric path.

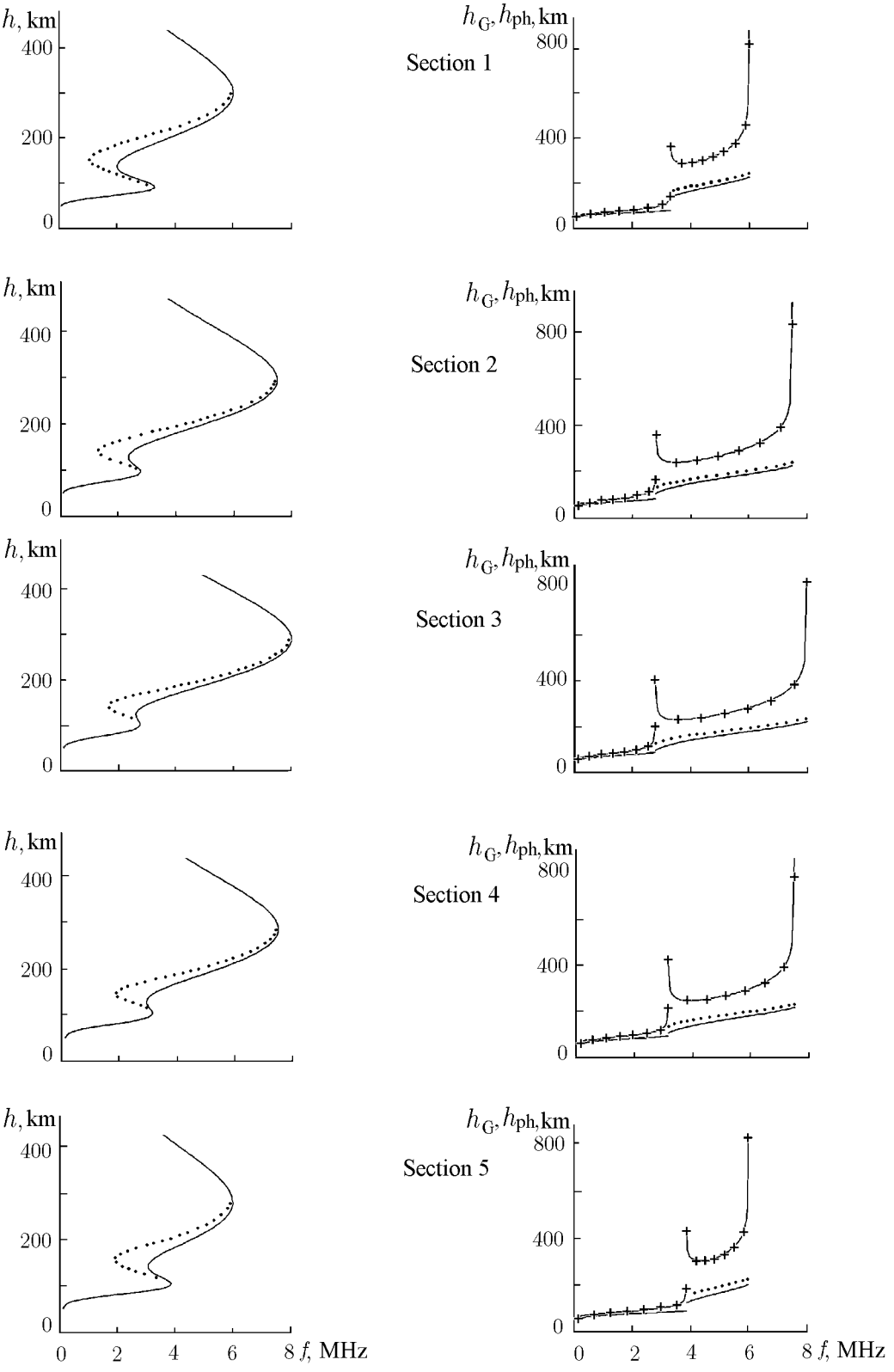

Fig. 5. PFP, group, and phase heights in the sections of a longitudinally inhomogeneous path.

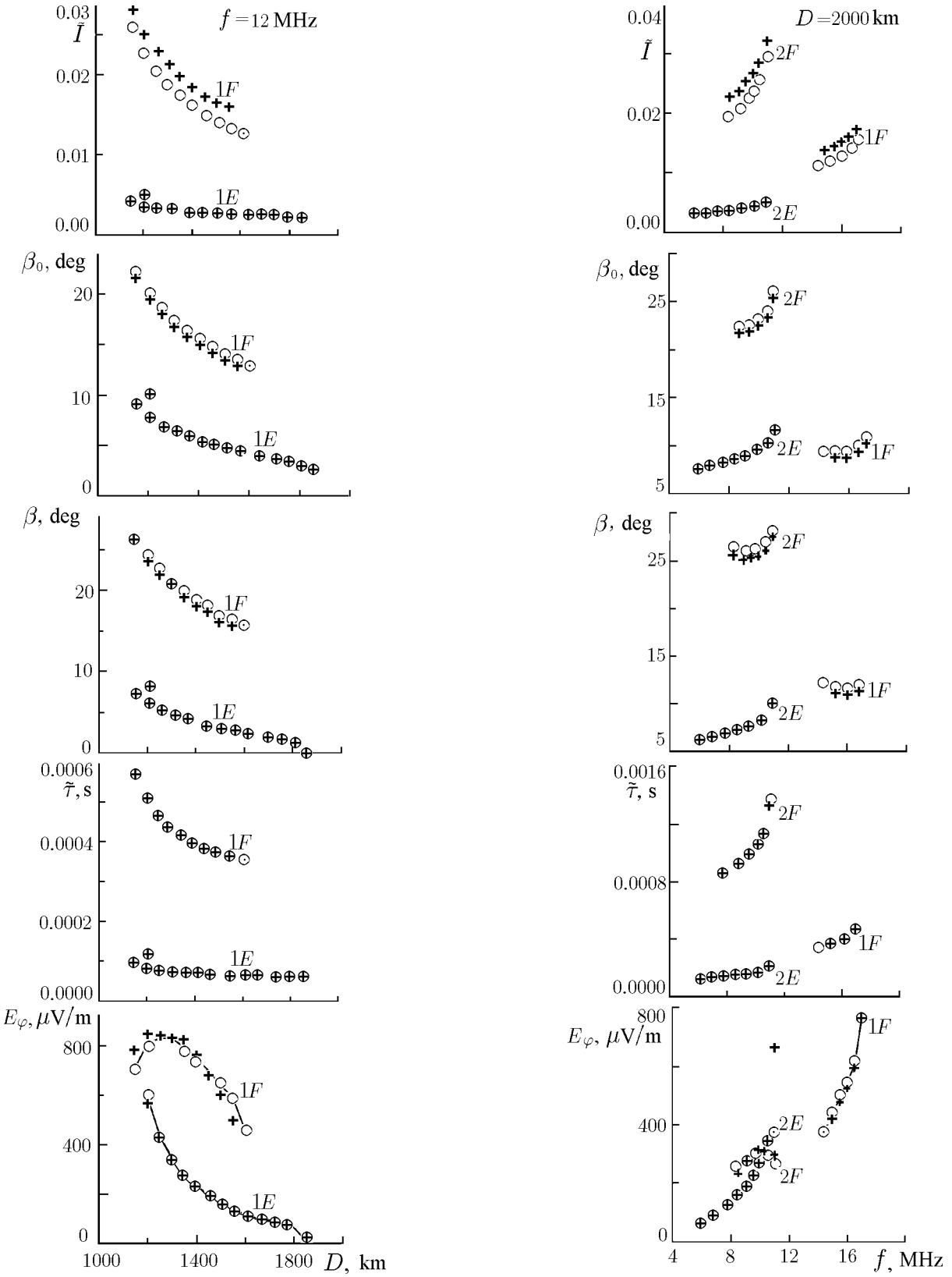

Fig. 6. Distance and frequency sweeps of the main characteristics on a longitudinally inhomogeneous path.

The use of ionosphere models, adapted by matching with HFC in the set of radio-path points, for diagnostics of the medium can lead to the reconstruction of media not belonging to the family of weakly discernible ones in the characteristics of an obliquely propagating signal and precluding agreement with oblique ionosphere sounding data. Satisfactory results in this method of reconstruction of media can be obtained by adapting ionosphere models simultaneously to vertical and oblique sounding data.

It becomes possible to fix the valley unambiguously with the shape postulated when the anisotropy of the ionosphere is taken into account and the PFP is reconstructed from the HFC of ordinary and extraordinary magneto-ionic signal components [15, 16]. However, the extraordinary component often is not recorded because of its low level, and the use of this method is restricted by the lack of measurement data.

In modern diagnostic facilities, the shortcomings of certain PFP reconstruction methods is compensated by combining different methods.

REFERENCES

1. P. Bentse, I. Shaiko, and G. Shatori, in: *Methods of Calculation and Study of Ionospheric $N(h)$-Profiles* [in Russian], IZMIRAN, Moscow (1973), pt. 1, p. 37.
2. T. L. Gulyaeva, in: *Methods of Calculation and Study of Ionospheric $N(h)$-Profiles* [in Russian], IZMIRAN, Moscow (1973), pt. 1, p. 76.
3. J. E. Titheridge, *Technical Report of RRC of Univ.*, Auckland, No. 78/1a, New Zealand (1978).
4. S. Ya. Mikhailov, *Studies in Geomagnetism, Aeronomy, and Solar Physics* [in Russian], Sib. Br. RAS Publishers (1978), No. 109, pt. 1, p. 196.
5. S. Ya. Mikhailov, *Method for calculation of the spatio-frequency distribution of HF signal characteristics in a three-dimensional inhomogeneous ionosphere, based on the waveguide approach: Ph. D. Thesis* [in Russian], Irkutsk (1993).
6. Yu. N. Dnestrovsky and D. P. Kostomarov, *Geomagn. Aéronom.*, 6, No. 1, 138 (1966).
7. V. B. Ivanov and A. N. Lapshin, in: *Proc. of the Mathematical Regional Scientific Conference "Radiophysics and Electronics: Problems in Science and Teaching," dedicated to the 100th anniversary of invention of radio* [in Russian], Institute of Solar–Terrestrial Physics, Sib. Br. RAS, Irkutsk (1995).
8. J. E. Jackson, *J. Geophys. Res.*, **61**, 107 (1956).
9. V. P. Modenov, *Dokl. Akad. Nauk*, **296**, No. 3, 536 (1987).
10. G. Korn and T. Korn, *Handbook of Mathematics* [Russian translation], Nauka, Moscow (1968).
11. S. Ya. Mikhailov, *Studies in Geomagnetism, Aeronomy, and Solar Physics* [in Russian], Nauka, Moscow (1989), No. 84, 177.
12. V. L. Ginzburg, *Propagation of Electromagnetic Waves in Plasmas* [in Russian], Nauka, Moscow (1960).
13. T. Kobayashi, *J. Rad. Res. Labs.*, **8**, No. 40, 395 (1961).
14. S. Ya. Mikhailov and A. P. Potekhin, *Studies in Geomagnetism, Aeronomy, and Solar Physics* [in Russian], Nauka, Moscow (1987), No. 77, p. 29.
15. I. Kutiev, *Methods for Calculation and Study of Ionospheric $N(h)$-Profiles* [in Russian], IZMIRAN, Moscow (1973), pt. 1, p. 12.
16. N. P. Danilkin and O. A. Mal'tseva, *Ionospheric Radio Waves* [in Russian], Rostov Univ. Press (1977).